# [Re] Predicting metabolic biomarkers of human inborn errors of metabolism

**Thierry D.G.A. Mondeel**[1,*], **Vivian Ogundipe**[2], **and Hans V. Westerhoff**[1, 3, 4]

**1** Synthetic Systems Biology and Nuclear Organization, Swammerdam Institute for Life Sciences, University of Amsterdam, The Netherlands **2** Department of Cell Biology, University Medical Center Groningen, University of Groningen, The Netherlands **3** Molecular Cell Physiology, Amsterdam Institute for Molecules, Medicines and Systems, VU University Amsterdam, The Netherlands **4** Manchester Centre for Integrative Systems Biology, School of Chemical Engineering and Analytical Science, The University of Manchester, UK

d.g.a.mondeel@uva.nl (thierry.mondeel@gmail.com)

> **A reference implementation of**
>
> → T. Shlomi, M.N. Cabili, E. Ruppin, Predicting metabolic biomarkers of human inborn errors of metabolism, Mol. Syst. Biol. 5 (2009) 263. doi:10.1038/msb.2009.22.

## Introduction

Shlomi et al. [7] have developed a way in which flux variability analysis [3] is used to predict biomarkers for inborn errors of metabolism (IEMs). The approach focuses on exchange reactions in a metabolic network that connect extracellular metabolites that reside in a medium, which might correspond to the blood, to a reservoir such as the urine. The method then determines the ranges of exchange fluxes that are compatible with constraints set by the network's topology, flux bounds of reactions and the requirement of steady state for each metabolite. Shlomi et al. proposed that if any such ranges shift convincingly when the network contains a mutation, the concentration ranges of the corresponding metabolites in the reservoir should shift in parallel and these metabolites would therefore be biomarkers.

Shlomi et al. illustrated the method first on a virtual metabolic map and further validated their technique using the reconstruction of the human metabolic map Recon1 [1] empirically with respect to known biomarkers, but did not provide any formal proof. For a set of 17 IEMs that affect amino acid metabolism, they found 56% of the biomarkers that are correctly predicted and 76% of predicted biomarkers that were predicted correctly in terms of whether they increased or decreased in concentration. Thiele et al. [9] later found an even higher precision using essentially the same FVA methodology on an updated version of the metabolic reconstruction.

Below, we first introduce the essential vocabulary and concepts necessary for understanding the method proposed by Shlomi et al.

### Definitions

Exchange reactions are reactions in the metabolic network that allow import and/or export of metabolites from the metabolic map. Exchange reactions are represented by

non-mass-balanced pseudoreactions, e.g. $X \leftrightarrow \varnothing$. Positive flux indicates net secretion of $X$ by the cell and negative flux indicates the net uptake of $X$.

We define boundary metabolites to be metabolites that are involved in exchange reactions with the environment, i.e. they serve as inputs and/or outputs for the metabolic network, e.g. glucose and $CO_2$. These metabolites typically exist both inside and outside the cell.

Each boundary metabolite will be associated with the range of flux its exchange reaction supports under the following constraints for the flux distributions in the model: (i) network topology, (ii) mass-balance for all metabolites, (iii) flux bounds of reactions in the network. Optionally, there is an additional constraint of being optimal with respect to attaining or maximizing a certain set of fluxes, the "objective", in the model.

Biomarkers are those boundary metabolites the range of exchange flux of which differs between the wild-type (WT) and mutant simulations. Shlomi et al. proposed a threshold of at least 10% difference in the lower or upper bounds of the wild-type vs. the mutant flux intervals.

Each biomarker will be associated with a prediction for being either elevated or decreased in the mutant case, as compared to the wild type. A biomarker is considered to have an increased, or reduced, extracellular concentration in the mutant case if, when plotting the wild-type and mutant flux-variability intervals on a horizontal axis, both the lower and upper boundary of the mutant interval are shifted to the right, or left, respectively (see Figures 2B and 3B). If the two borders of the mutant interval move in opposite directions with respect to the wild-type interval, the result is scored as 'unchanged' and the boundary metabolite is not considered to be a biomarker.

### Flux variability calculations

Flux ranges for boundary metabolites, consistent with the requirements of a steady state and constraints on reaction reversibilities, may be calculated by applying flux variability analysis [3]. Mathematically, flux variability analysis for a specific exchange reaction $v_i$ entails the following linear programming problem:

$$\text{Min } v_i \text{ or Max } v_i, \text{ such that for all } k$$
$$\boldsymbol{S}\boldsymbol{v} = \boldsymbol{0}$$
$$Z \geq \phi Z_{\max}$$
$$\alpha_k \leq v_k \leq \beta_k \tag{1}$$

Here $\boldsymbol{v}$ is the column vector of fluxes representing all reactions in the model, $v_i$ is the flux of the exchange reaction of a given boundary metabolite $i$, $\alpha_k$ is the, possibly negative, lower bound for reaction $k$ and similarly $\beta_k$ is the, possibly negative, upper bound for reaction $k$. The reaction bounds are the $V_{max}$'s of the reactions and are part of the metabolic network definition, typically they are set to either 0 or $\pm 1000$ if the true, biological, $V_{max}$'s are not known. These values allow specification of irreversible reactions by setting the lower bound (or upper bound) to zero. The index $i$ specifies a single reaction that is to be maximized, whereas the index $k$ is used to index the bound constraints that exist for each reaction, including $v_i$. $v_i$ may be maximized in the forward (positive flux) or the reverse (negative flux) direction if allowed by the bounds on $v_i$. For a network with $m$ metabolites and $r$ reactions, i.e. fluxes, $\boldsymbol{S}$ is the stoichiometry matrix for the network of size $m \times r$. The numeric, typically integer, elements of $\boldsymbol{S}$ represent the stoichiometry coefficients of each metabolite $m$ in each reaction $r$. $Z = \boldsymbol{c}^T \boldsymbol{v}$ is the objective function defined for the map, entailing a linear combination, defined by column vector $\boldsymbol{c}$, of one or more reactions. The vector $\boldsymbol{c}$ is an indicator of objective reactions, i.e. it contains a value of 1 in rows corresponding to fluxes that are to be included in the objective, and zeros in all other rows. Due to

the vector multiplication $\boldsymbol{c}^T \boldsymbol{v}$, the objective $Z$ sums the fluxes of the reactions that correspond to rows containing a value of 1 in $\boldsymbol{c}$. $Z_{\max}$ denotes the maximal value of the objective function. We define $0 \leq \phi \leq 1$ to be an arbitrary minimal fraction of the maximal objective function value that has to be achieved. When $\phi = 1$ we ask for the range of flux allowed for reaction $v_i$ while maintaining the maximal value of the linear combination of objective fluxes. When setting $\phi = 0$, one is asking for the allowable flux range through reaction $v_i$ regardless of the value of the objective function (although the sign has to be maintained). The latter, i.e. $\phi = 0$, is the case considered in the method by Shlomi et al. The choice of $\phi$ matters because when $\phi \neq 0$ we are requiring flux to flow through the set of objective reactions (unless $Z_{\max} = 0$). This may entail a forced directionality through reactions that are required to ultimately produce flux in the objective reactions. These additional limitations in the freedom of the flux pattern may subsequently impact the biomarker predictions. The approach discussed here entails predictions purely based on the network topology and therefore sets $\phi = 0$.

### Reference implementation

The source code for the original publication is not publicly available and the computation environment used was not mentioned in the publication. The [MATLAB COBRA toolbox](#) contains code to reproduce the analysis by Thiele et al. but this was also performed in MATLAB.

We here present an implementation of the biomarker prediction method originally proposed by Shlomi et al., programmed in Python, and reproduce the results presented in Figure 1A-B, 2 and 3 of the original publication. These figures concern the method's application to a simple metabolic map and then to a set of 17 amino acid metabolism disorders. Our Python module provides the biomarker prediction algorithm and is agnostic of the map used. It can therefore be applied to other maps than the human metabolic reconstruction considered by Shlomi et al. Jupyter notebooks are provided that generate the illustrative map and reproduce all results referred to in Figures 1A-B, 2 and 3 of Shlomi et al. Our implementation is based on information given in the original paper. However, some details critical to the reproduction were left unexplained there and are highlighted here. We also include a more detailed discussion of one of the amino acid IEMs to examine the robustness of the predictions made using this approach. We feel this adds to the utility of this reference implementation and the understanding of the approach introduced by Shlomi et al.

## Methods

### Overview

We implemented the method of Shlomi et al. in Python. Our Python function has several input parameters, most of which are optional in order to enable the user to perturb the network in various ways and to try variations of the method that differ from the ones implemented here or in Shlomi et al. The default settings are such that they mimic the approach Shlomi et al. originally proposed. All flux-variability analyses are performed using COBRApy [2].

All simulations discussed here were performed in Python 3.6 using COBRApy [2] (version 0.9) and Pandas (version 0.20.3). This repository also functions in conjunction with [MyBinder](#) which allows for full reproducibility in the 'cloud' without any need for installation of additional software.

The rest of this section introduces the approach proposed by Shlomi et al. as we implemented it.

## Implementation of the algorithm

Here, we examine inborn errors of metabolism (IEMs) resulting from loss-of-function mutations in a single enzyme $r$ that may catalyse multiple chemical reactions. For IEMs that disrupt the activity of several reactions, Shlomi et al. proposed applying the approach to each reaction individually and then combining the list of biomarkers.

Therefore, for a given IEM we loop the following sequence of steps for each affected reaction $r$ and for each boundary metabolite $m$:

1. Compute the exchange flux interval of $m$, when $r$ is forced to be active with a flux of at least $\epsilon \geq 0$. By default $\epsilon = 1$. We refer to this as the forward wild-type interval $WT_{r,m}^+$.
2. For reversible reactions $r$, if the forward interval yields a flux range of $[0,0]$, constrain the flux to be negative and lower than $-\epsilon \leq 0$, and compute the backward wild-type interval $WT_{r,m}^-$.
3. The wild-type interval $WT_{r,m}$ is equal to the union of the forward and backward intervals.
4. Compute the exchange flux interval of $m$ when $r$ is forced to be inactive by temporarily setting the lower and upper bound of $r$ to zero. This interval is denoted by $M_{r,m}$.
5. Compare the wild-type and mutant intervals and predict whether the external concentration of $m$ increases, decreases or remains unchanged when reaction $r$ is forced to be inactive. This is done by the following rule: if both boundaries are higher in the mutant simulation than the corresponding boundaries in the wild-type simulation, then $m$ is predicted to be a biomarker and elevated. If both boundaries are lower in the mutant simulation as compared to the wild-type simulation, then the metabolite is predicted to be a biomarker and reduced. If the predicted changes are smaller than 10%, $m$ is a low confidence biomarker. When the wild-type and mutant intervals are disjoint intervals, $m$ is a highly confident (H.C) biomarker.

After the loop (steps 1-5) is completed, contradictory predictions for $m$ between the affected reactions $r$ are dealt with based on a majority rule. When there is an equal number of elevated and reduced predictions, the boundary metabolite is considered to be unchanged, i.e. not a biomarker.

The flux variability analyses that yield the exchange flux intervals computed in step 1, 2 and 4 are handled by the flux_analysis.variability.flux_variability_analysis function in Cobrapy. The input for this function comprises the model, along with its associated flux bounds which change during step 1, 2 and 4, the list of reactions for which to calculate the flux intervals and a fraction of the optimal objective flux to minimally obtain (fraction_of_optimum). In our case we pass the model with flux bounds as described above, lists of exchange reactions for the metabolites of interest and a fraction of optimum of zero.

# Results

In this section we start with an analysis of the sensitivity of the method which was not clearly discussed in the original publication but is easily facilitated with our reference implementation. Subsequently, we discuss the reproduction of Figures 1, 2 and 3 from the original publication.

## Robustness of the flux variability method

Shlomi et al. did not discuss in detail the effects of changing various parameter settings of, and assumptions inherent to, their FVA-based method, nor did they present a proof
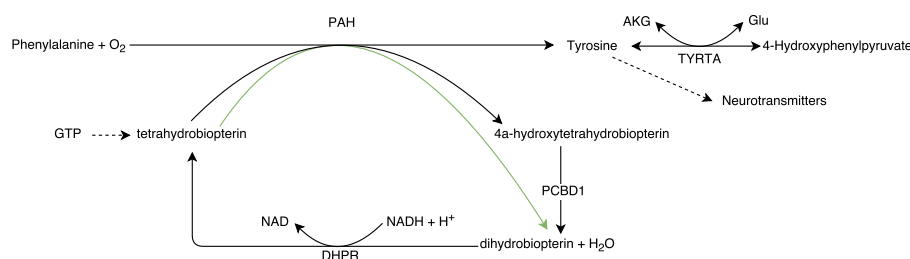
**Figure 1:** Scheme of the network surrounding phenylalanine hydroxylase (PAH) and its cofactors. The 4a-hydroxytetrahydrobiopterin produced by PAH may spontaneously or when catalysed by PCBD1 (EC 4.2.1.96) dehydrate to dihydrobiopterin which may be enzymatically reduced back by $NADPH + H^+$ to tetrahydrobiopterin through DHPR (EC 1.5.1.34). The solid black lines indicate reactions that are contained in both Recon 1 and Recon 2.2 [8]. The solid green line refers to the alternative PAH reaction that includes the spontaneous dehydradation towards dihydrobiopterin that is only present in Recon 2.2. Dashed lines indicate sources of the synthesis pathways or terminal products of the indicated metabolites. The tyrosine transaminase (TYRTA) uses oxoglutarate (AKG) and glutamate (Glu) as cosubstrates.

of any generality. Because our Python implementation allows the user to set various parameters, it becomes possible to illustrate how specific settings in the approach proposed by Shlomi et al. affect the outcome of the simulations. An example of the potential pitfalls and issues with this method is investigated below, in which we look at predictions for the inborn error of metabolism known as Phenylketonuria (PKU). Here, we simulate this disease by applying one of its potential causes, i.e. dysfunctionality of the enzyme converting phenylalanine into tyrosine.

PKU patients are known for elevated levels of phenylalanine and decreased levels of tyrosine in their serum. We illustrate this briefly in an example also considered in Figure 2 of Shlomi et al. In Figure 1, we sketched some essential features of the metabolic network surrounding the phenylalanine hydroxylase (PAH) enzyme that malfunctions in PKU. Unless stated otherwise, the simulations are performed with a medium that allows efflux through all exchange reactions with an upper bound of 1000 and influx through all exchange reactions with a lower bound of −1 and we use the default settings, including a 10% significance threshold. The only considered biomarkers are the 20 proteinogenic amino acids. We will consider six cases in total. The results are summarized in Table 1.

Perhaps the most fundamental question is: can changes in network topology result in different predictions? The answer is yes. One illustration of this is the comparison of predictions between Recon 1 and Recon 2. As Table 1 indicates, using the same medium and algorithm settings for both Recon 1 and Recon 2.2, the two networks led to different predictions of the effect of a defect of phenylalanine hydroxylase on tyrosine. The application of the flux variability method to Recon 1 correctly predicted both tyrosine and phenylalanine as biomarkers as well as the directionality of the change in their concentrations. In contrast, the prediction based on Recon 2.2 fails to identify tyrosine as a biomarker.

With ever-improving network annotations, it becomes feasible to simulate the gene knockout directly for most single gene defects leading to inborn errors of metabolism. Shlomi et al. directly blocked or activated reactions associated with a causal gene for a specific IEM. For enzymes partaking in several reactions, Shlomi et al. proposed activating and blocking all reactions associated with the gene individually and then taking the union of their predicted biomarkers. A majority rule was applied when a biomarker was subject to qualitatively different predictions between the enzyme-catalyzed reactions encoded by the gene. We will refer to this as the asynchronous setting. Blocking all affected reactions simultaneously could yield different predictions.
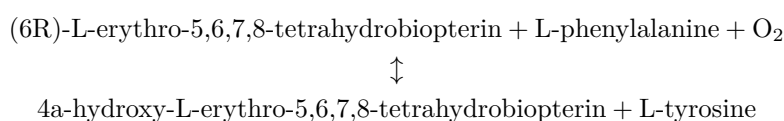
We will refer to this as the synchronous setting. In our implementation, we added the option to choose between the asynchronous and synchronous setting.

For example, consider a gene that encodes an enzyme that catalyzes two chemically different reactions, $R_1$ and $R_2$. Using the asynchronous setting, we would run the algorithm once for $R_1$ and once for $R_2$ and take the union of all predicted biomarkers. Inconsistent predictions between $R_1$ and $R_2$ are dealt with based on a majority rule (see Methods). In contrast, with the synchronous setting, we would run the algorithm once. For the wild-type simulation, we would simultaneously force flux through both reactions and in the mutant simulation, we would block both reactions. The synchronous approach simulates the complete catalytic inactivity or absence of the enzyme and therefore the infeasibility of any reactions it catalyzes. This corresponds to a deletion of the gene. The asynchronous approach might correspond to a point mutation that changes the specificity of the enzyme.

**Table 1:** Summary of predictions made using the FVA-based biomarker prediction method for the inborn error of metabolism phenylketonuria for two networks ($R_1$ = Recon 1 and $R_2$ = Recon 2), with or without the synchronous setting (indicated by "sync" here) and with high (maximum influx of 20) or low (no influx) hydroxyphenylpyruvate (hpp +/-) in the medium. $^*$ refers to a situation without any tyrosine production in the mutant simulation. $^{**}$ refers to the situation where tyrosine reduction is so small that it does not reach the 10% threshold. '-' indicates no prediction because the boundaries did not change from wild-type to mutant. $\epsilon = 0$ refers to the case where we do not force any flux through the affected reaction(s) in the wild-type simulation. In all other columns, $\epsilon = 1$. The full output with interval bounds that the method generated can be found in the relevant notebook in this repository.

| Biomarker | $R_1$ | $R_2$ | $R_2$ sync | $R_2$ hpp$-$ | $R_2$ hpp$+$ | $R_1$ $\epsilon = 0$ |
|---|---|---|---|---|---|---|
| Phenylalanine | Elevated | Elevated | Elevated | Elevated | Elevated | - |
| Tyrosine | Reduced | - | Reduced | Reduced* | Reduced** | Reduced |

Returning to the example of phenylketonuria, we simulated this for Recon 2.2 using the synchronous approach. Column 3 in Table 1 shows that the result now agrees with the Recon 1 asynchronous predictions. Using Recon 1, we came to the correct prediction because it contains only one reaction ('PHETHPTOX2') linked to the PKU gene, i.e. only phenylalanine hydroxylase (Entrez ID: 5053, HGNC:8582):

$$(6R)\text{-L-erythro-5,6,7,8-tetrahydrobiopterin} + \text{L-phenylalanine} + O_2$$
$$\updownarrow$$
$$4a\text{-hydroxy-L-erythro-5,6,7,8-tetrahydrobiopterin} + \text{L-tyrosine}$$

In Recon 1, the 4a-hydroxytetrahydrobiopterin produced may dehydrate to 6,7-dihydrobiopterin by the action of the 'THBPT4ACAMDASE' reaction catalyzed by the PCBD1 enzyme (EC 4.2.1.96). Recon 2.2 contains, in addition to the PAH and PCBD1 catalyzed reactions indicated above, the overall reaction where the spontaneous dehydration reaction is included, again attributed to phenylalanine hydroxylase:

$$(6R)\text{-L-erythro-5,6,7,8-tetrahydrobiopterin} + \text{L-phenylalanine} + O_2$$
$$\updownarrow$$
$$6,7\text{-dihydrobiopterin} + \text{L-tyrosine} + H_2O.$$
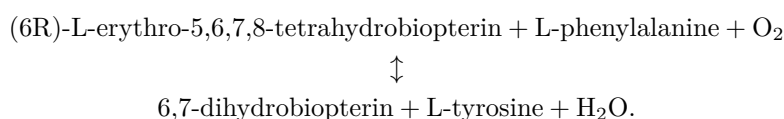
These details are included in the pathway summary in our Figure 1. When the reactions affected by the PKU gene are knocked out simultaneously, Recon 2 correctly predicts both tyrosine and phenylalanine as biomarkers. When blocking only one

reaction, there is a way to produce tyrosine. Consequently, tyrosine is not predicted as a biomarker if Recon 2 is used as the metabolic map.

Another significant modulation point for the method, and for flux-balance-based models in general, is the medium. More specifically, it matters for the biomarker prediction which other exchange reactions are allowed to have a non-zero flux and what the bounds on these fluxes are. Changes in this leave the internal network topology unchanged and instead alter how the model is allowed to interface with biological compartments or environments that are not explicitly modeled. This potentially has major consequences, as it may open up or shut down entire parts of the metabolic network that rely on specific substrates. Additionally, it interacts with the significance threshold, since the medium components together with the network pathways (and their $V_{max}$'s) determine the amount of a given metabolite that may be produced.

In order to examine these ramifications, we continue with the synchronous PKU example and note that tyrosine production flux goes down in the mutant simulation, but not to zero. This is due to an alternative tyrosine synthesis pathway in the model originating from 4-Hydroxyphenylpyruvate in the medium through the 'TYRTA' reaction (tyrosine transaminase E.C. 2.6.1.5). This transaminase is considered to be reversible in Recon 2 and Equilibrator [5] annotates this reaction with a $K'_{eq} \approx 1$. It should be mentioned, however, that the ability for transport of hydroxyphenylpyruvate is speculative. Column 4 and 5 in Table 1 show the results when using the standard medium and a medium without or with increased (i.e. influx at -20) 4-Hydroxyphenylpyruvate influx respectively. In FBA and FVA, changes in medium concentrations of exchange metabolites are modelled by changing the corresponding influx (inward exchange) $V_{max}$ (bound). In the former, the ability to produce tyrosine indeed disappears in the mutant case. In the latter, there is so much leftover capacity that the change in interval bounds slips below the 10% cutoff. This sensitivity to medium composition appropriately reflects the phenomenon of cells behaving differently in different culture media, and organisms behaving differently depending on their nutrition. Our discussion here may highlight that this feature should be expected to affect the pertinence of biomarkers. Biomarkers may have a tendency to be non-robust, dependent as they can be on network topology details and nutrition.

Finally, we consider the value of the $\epsilon$ parameter, which indicates the amount of flux forced through the reaction in the wild-type condition. The last column in Table 1 indicates that phenylalanine does not show up as a biomarker if setting $\epsilon = 0$ and the PKU simulation is performed on Recon 1. This may also be the reason why Sahoo et al. did not manage to find phenylalanine as a biomarker for PKU in their study [6].

## Reproduction of Figure 1 panel A and B in [7]

The original publication's Figure 1, panel A and B, exemplified the biomarker prediction method for an illustrative network. It is reproduced here as Figure 2. The simple nature of the example serves to explain the reasoning behind the method and also helped us validate our implementation of the method. This repository provides an SBML file of the network, the Jupyter notebook that generates it and a Jupyter notebook reproducing the biomarker prediction. The image itself was produced using Adobe Illustrator.

The network in Figure 2A consists of seven metabolites, 6 of which (i.e. all except M3) have exchange reactions. We consider a hypothetical deletion of the enzyme catalyzing the conversion of M1 into M2 coupled to the conversion of M3 into M4. Shlomi et al. graphically provide the biomarker prediction for this network in their Figure 1A. Here, we do so graphically and numerically in Figure 2B and this paper is accompanied by a Jupyter notebook reproducing the biomarker prediction. In our analysis, all exchange reactions were given inward bounds of $-10$ and outward bounds of $+1000$ so that the internal reaction bounds (of $\pm1000$) are never reached. Figure 2B shows that all exchangeable metabolites except M5 and M7 are predicted to be
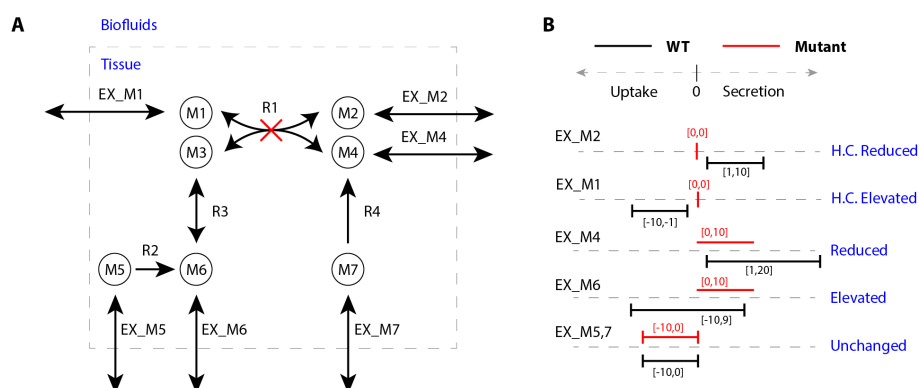
**Figure 2:** (A) A metabolic network used to illustrate the predictions of biomarkers of IEMs as originally considered in the work by Shlomi et al. for their prediction of biomarkers of IEMs. All metabolites but M3 have an exchange reaction allowing for uptake or secretion of the metabolites. M2 synthesis is fully dependent on uptake of M1 and M5 or M6. The IEM considered is one that leads to deletion of the enzyme converting M1 plus M3 to M2 plus M4. (B) Visual illustration of the predicted exchange intervals for each of the metabolites with an exchange reaction. The wild-type (WT) interval is indicated in black, the mutant interval in red. Each interval is associated with a numeric interval predicted by the biomarker prediction algorithm and with a qualitative prediction for the level of the metabolite in the biofluids (see methods). H.C. is an abbreviation for a highly confident biomarker, see main text.

robust biomarkers.

The exchange interval we found for metabolite M6 shows that in the wild-type case, M6 can be either taken up from biofluids or secreted. The upper bound is lower in absolute value than the lower bound because in the wild type, at least 1 unit of flux is needed to provide M3 as substrate for the enzyme under investigation since the enzyme convert M1 and M3 to M2 and M4 is required to have a minimal flux of 1 unit. In the disease case, M6 (synthesized through M5) can only be secreted to biofluids. These results are in full agreement with the original publication.

## Reproduction of Figure 2 in [7]

Shlomi et al. applied their method to the reconstructed human metabolic map, examining a set of 17 IEMs affecting amino-acid metabolism. Figure 2 in their publication compares predicted biomarkers with known biomarkers from the OMIM database [4]. We reproduced the analysis for each IEM listed in Table 2 and ultimately found full agreement between what was reported by Shlomi et al. and the results of our implementation.

It is worthwhile to note, with an eye on the sensitivity of this approach to the various settings, that we needed to set the medium composition very specifically. Shlomi et al. did not report on their chosen medium in their publication but we were able to reproduce their results by setting all inward flux bounds to $-10$ and all outward flux bounds to 1000.

We made use of the Excel file included as supplementary information in [7] and included it in this repository as well. The genes and reactions linked to a given IEM are detailed in this Excel file. We attempted to extract the genes for each IEM and using the Recon 1 map, deduced the coupled reactions, but found out that this yielded predictions different from the ones presented by Shlomi et al. However, the reactions listed in the Excel file are not necessarily the same reactions that are linked in Recon 1 to the genes linked to the IEMs. Assuming the reconstruction of the metabolic network to be accurate, this raises some doubts as to the correctness of the results obtained by Shlomi et al. for those IEMs where the listed reactions did not agree with

the reconstructed map.

Additionally, we needed to manually add the information for S-Adenosylhomocysteine hydrolase and Methionine adenosyltransferase deficiency, since they were missing from the Excel file and to reduce the tetrahydrobiopterin deficiency gene list to only consider QDPR (quinoid dihydropteridine reductase). Lastly, Histidinemia was in the Excel file associated to the reaction HISD whereas this should have referred to HISDr to match the reaction identifier in Recon 1. After these changes, we recovered the results as originally presented and as summarized here in Table 2.

**Table 2:** We used our implementation to reproduce the biomarkers for the list of inborn errors of metabolism shown in Figure 2 in [7]. Using the supplementary Excel table of [7] linking IEMs to causative genes and affected reactions, we filtered out those that are listed here. The only considered biomarkers are the 20 proteinogenic amino acids. We report all biomarkers the change of which exceeds the 10% threshold and categorize them by their qualitative prediction: elevated or reduced serum levels.

| IEM | Affected reactions | Elevated | Reduced |
|---|---|---|---|
| S-Adenosylhomocysteine hydrolase | SEAHCYSHYD, AHCi | L-Methionine | L-Cysteine |
| Alkaptonuria | HGNTOR | L-Tyrosine | |
| Argininemia | ARGN | | |
| Cystinuria | CYSTSERex, SERLYSNaex | | |
| Lysinuric protein intolerance | SERLYSNaex | | |
| Glutamate formimino-transferase deficiency | FTCD, GluForTx | L-Histidine | |
| Histidinemia | HISDr | L-Histidine | |
| Homocystinuria | CYSTS, MTHFR3, METS | L-Methionine | L-Cysteine |
| Hyperprolinemia type I | PRO1xm, PROD2m | | |
| Maple syrup urine disease | OIVD1m, OIVD2m, OIVD3m | L-Valine, L-Isoleucine L-Leucine, | |
| Methionine adenosyl-transferase deficiency | SELMETAT, METAT | L-Methionine | L-Cysteine |
| methylmalonic acidemia | CBLATm, CBL2tm, MMMm | L-Isoleucine | |
| Phenylketonuria | PHETHPTOX2 | L-Phenylalanine | L-Tyrosine |
| Phenylketonuria II | DHPR | | |
| Tyrosinemia type I | FUMAC | L-Tyrosine | |
| Tyrosinemia type III | PPOR, 34HPPOR | L-Tyrosine | |
| Glycine encephalopathy | GCC2am, GCC2bim, GCC2cm, GCCam, GCCbim, GCCcm | | |

## Reproduction of Figure 3 [7]

Figure 3 in the original publication entailed an in-depth look at the effect of inborn errors in AHCY and CBS on methionine metabolism. We reproduced this Figure as Figure 3. We used Adobe Illustrator to redraw the network from the original publication and based the intervals in panel B on the numerical results the algorithm predicts. The qualitative results are already contained in 2. The numerical results illustrated in 3B may be reproduced using the notebook *Repro-*
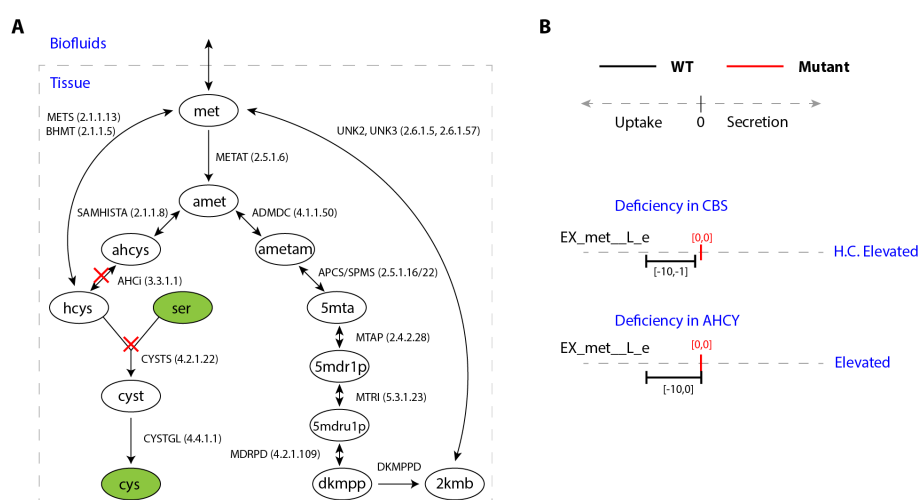
**Figure 3:** Reproduction of Figure 3 in [7]. (A) Illustration of the subnetwork of Recon 1 relevant to the effect of homocystinuria on the metabolism and transport of methionine. Nodes represent metabolites and edges represent reactions. For simplicity, only abbreviations of metabolite names are given in the figure. The full names are: L-Methionine (met), S-Adenosyl-L-methionine (amet), S-Adenosyl-L-homocysteine (ahcys), L-Homocysteine (hcys), L-Serine (ser), L-Cystathionine (cyst), L-Cysteine (cys), S-Adenosylmethioninamine (ametam), 5-Methylthioadenosine (5mta), 5-Methylthio-5-deoxy-D-ribose 1-phosphate (5mdr1p), 5-Methylthio-5-deoxy-D-ribulose 1-phosphate (dmdru1p), 2,3-diketo-5-methylthio-1-phosphopentane (dkmpp), 2-keto-4-methylthiobutyrate (2kmb). Metabolites with a green background color participate in additional reactions not shown here. Reactions are indicated by their identifiers in Recon 1 and with a corresponding enzyme commision number if available. We highlighted the mutations for Homocystinuria (dysfunctional CBS) and hypermethioninemia (dysfunctional AHCY). (B) Prediction of concentration changes of methionine in homocystinuria and S-adenosylhomocysteine hydrolase deficiency based on the biomarker prediction algorithm. The wild-type (WT) interval is indicated in black, the mutant interval in red. Each interval is associated with a numeric interval predicted by the biomarker prediction algorithm and with a qualitative prediction for the level of the metabolite in the biofluids (see methods). H.C. is an abbreviation for a highly confident biomarker, see main text.

*duce_figure_2_and_3_Shlomi2009.ipynb.* For clarity we included a section in the notebook that details the results relevant to Figure 3B.

We note that in early versions of this reproduction we were utilising a medium that allowed influx of $-1$ for all medium components, as opposed to $-10$ now. It turns out that a setting of $-1$ does accurately reproduce the results for Figure 2, but not for Figure 3. For the CBS IEM the WT interval would correspond to $[-1, -1]$ and would therefore be a point instead of a wide interval as Shlomi et al. draw it. We included this simulation in the last cell of the notebook *Reproduce_figure_2_and_3_Shlomi2009.ipynb* This is another example of the inherent sensitivity of the approach to various settings in the algorithm.

## Conclusion

The results summarized in Figures 1 (panel A and B), 2 and 3 of [7] have been successfully replicated with the software tools provided here. Overall, the reproduction process went smoothly, since the method was applied to both an illustrative example and to the human metabolic reconstruction, resulting in a multitude of test cases for the implementation.

The obstacles we encountered were the lack of explicit discussion on the set of fluxes allowed into and out of the model and a set of discrepancies between the gene-reaction mappings listed in the supplementary Excel file and the actual gene-reaction mappings in the metabolic network. However, trial and error and manual curation solved these issues.

We hope this reference implementation is useful to the community and can serve as a starting point for further implementations of this approach and serves as a warning of the accompanying sensitivities to various algorithm settings we have lain out in this manuscript.

## References

[1]   Natalie C. Duarte et al. "Global reconstruction of the human metabolic network based on genomic and bibliomic data." In: *Proceedings of the National Academy of Sciences of the United States of America* 104.6 (Feb. 2007), pp. 1777–1782. ISSN: 0027-8424. DOI: 10.1073/pnas.0610772104.

[2]   Ali Ebrahim et al. "COBRApy: COnstraints-Based Reconstruction and Analysis for Python". In: *BMC Systems Biology* 7.1 (2013), p. 74. ISSN: 1752-0509. DOI: 10.1186/1752-0509-7-74.

[3]   R. Mahadevan and C. H. Schilling. "The effects of alternate optimal solutions in constraint-based genome-scale metabolic models". In: *Metabolic Engineering* 5.4 (2003), pp. 264–276. ISSN: 10967176. DOI: 10.1016/j.ymben.2003.09.002.

[4]   Victor A McKusick. "Mendelian Inheritance in Man and Its Online Version, OMIM". In: *The American Journal of Human Genetics* 80.4 (Apr. 2007), pp. 588–604. ISSN: 00029297. DOI: 10.1086/514346.

[5]   Elad Noor et al. "An integrated open framework for thermodynamics of reactions that combines accuracy and coverage." In: *Bioinformatics (Oxford, England)* 28.15 (Aug. 2012), pp. 2037–2044. ISSN: 1367-4811. DOI: 10.1093/bioinformatics/bts317.

[6]   Swagatika Sahoo et al. "A compendium of inborn errors of metabolism mapped onto the human metabolic network". In: *Molecular BioSystems* 8.10 (2012), p. 2545. ISSN: 1742-206X. DOI: 10.1039/c2mb25075f.

[7]   Tomer Shlomi, Moran N Cabili, and Eytan Ruppin. "Predicting metabolic biomarkers of human inborn errors of metabolism". In: *Molecular Systems Biology* 5.263 (Apr. 2009), p. 263. ISSN: 1744-4292. DOI: 10.1038/msb.2009.22.

[8]   Neil Swainston et al. "Recon 2.2: from reconstruction to model of human metabolism". In: (2016). DOI: 10.1007/s11306-016-1051-4.

[9]   Ines Thiele et al. "A community-driven global reconstruction of human metabolism." In: *Nature biotechnology* 31.5 (2013), pp. 419–425. ISSN: 1546-1696. DOI: 10.1038/nbt.2488.